HAL
open science

A Triple AGN in the NGC 7733-7734 Merging Group

Jyoti Yadav, Mousumi Das, Sudhanshu Barway, Francoise Combes

To cite this version:

Jyoti Yadav, Mousumi Das, Sudhanshu Barway, Francoise Combes. A Triple AGN in the NGC 7733-7734 Merging Group. Astronomy and Astrophysics - A&A, 2021, 651, pp.L9. 10.1051/0004-6361/202141210 . hal-03295889

HAL Id: hal-03295889

https://hal.sorbonne-universite.fr/hal-03295889

Submitted on 22 Jul 2021

HAL is a multi-disciplinary open access archive for the deposit and dissemination of scientific research documents, whether they are published or not. The documents may come from teaching and research institutions in France or abroad, or from public or private research centers.

L'archive ouverte pluridisciplinaire **HAL**, est destinée au dépôt et à la diffusion de documents scientifiques de niveau recherche, publiés ou non, émanant des établissements d'enseignement et de recherche français ou étrangers, des laboratoires publics ou privés.

Astronomy & Astrophysics manuscript no. main
June 24, 2021
©ESO 2021

Letter to the Editor

A Triple AGN in the NGC 7733–7734 Merging Group

Jyoti Yadav [1,2]⋆, Mousumi Das [1], Sudhanshu Barway [1], and Francoise Combes [3]

[1] Indian Institute of Astrophysics, Koramangala II Block, Bangalore 560034, India

[2] Pondicherry University, R.V. Nagar, Kalapet, 605014, Puducherry, India

[3] Observatoire de Paris, LERMA, College de France, CNRS, PSL University, Sorbonne University, F-75014 Paris, France

June 24, 2021

arXiv:2106.12441v1 [astro-ph.GA] 23 Jun 2021

ABSTRACT

Context. Galaxy interactions and mergers can lead to supermassive black hole (SMBH) binaries which become active galactic nuclei (AGN) pairs when the SMBHs start accreting mass. If there is a third galaxy involved in the interaction, then a triple AGN system can form.

Aims. Our goal is to investigate the nature of the nuclear emission from the galaxies in the interacting pair NGC 7733–NGC 7734 using archival VLT/MUSE Integral field spectrograph data and study its relation to the stellar mass distribution traced by near-infrared (NIR) observations from the South African Astronomical Observatory (SAAO).

Methods. We conducted near-infrared observations using the SAAO and identified the morphological properties of bulges in each galaxy. We used MUSE data to obtain a set of ionized emission lines from each galaxy and studied the ionization mechanism. We also examined the relation of the galaxy pair with any nearby companions with Far-UV observations using the UVIT.

Results. The emission line analysis from the central regions of NGC 7733 and NGC 7734 show Seyfert and LINER type AGN activity. The galaxy pair NGC 7733–34 also shows evidence of a third component, which has Seyfert-like emission. Hence, the galaxy pair NGC 7733–34 forms a triple AGN system. We also detected an Extended Narrow-line region (ENLR) associated with the nucleus of NGC 7733.

Key words. Galaxies: individual: NGC7733, NGC7734 – Galaxies: interactions – Galaxies: active – Galaxies: Seyfert – Galaxies: star formation – Techniques: imaging spectroscopy

1. Introduction

Galaxy interactions and mergers are the major drivers of galaxy evolution in our low redshift universe, leading to the growth of supermassive black holes (SMBHs), bulges, and massive galaxies (Di Matteo et al. 2005). One of the most favorable environments for such activity are galaxy groups where galaxies are closely interacting, especially those that have significant reservoirs of cold gas that can be used to fuel star formation and active galactic nuclear (AGN) activity (Eastman et al. 2007; Georgakakis et al. 2008; Arnold et al. 2009; Martini et al. 2009; Tzanavaris et al. 2014).

The tidal forces during galaxy interactions may trigger the formation of bars and spiral arms that produce gravitational torques on the stars and gas in the galaxy disks. These, in turn, drive gas into the nuclear regions, triggering central star formation (Springel et al. 2005; Hopkins & Quataert 2011). The gas accretion onto the SMBHs can trigger AGN activity, but the details of how the gas reaches the inner kpc region are still not clear. However, processes such as nuclear spirals and kpc-scale bars likely play an important role (Combes 2001). Observations suggest that most galaxies are associated with groups or have some companions (McGee et al. 2009). The galaxy interactions within the group can strongly affect the galaxy morphologies, and trigger star formation and AGN activity if the galaxies are gas-rich (Duc & Renaud 2013). Gas can also be pulled out due to tidal interaction and ram pressure stripping, as seen in the tails of HI gas or star-forming knots in Hα and ultraviolet (UV) (Kenney et al. 2004; von der Linden et al. 2010; Yadav et al. 2021).

As galaxies merge, the dynamical friction on the SMBHs in the individual galaxies causes them to move closer together. If the SMBHs are accreting, they can form AGN pairs (Rubinur et al. 2019). Studies show that there is a higher fraction of dual AGN in interacting galaxies, which indicates that galaxy interactions can trigger AGN activity (Satyapal et al. 2014; Kocevski et al. 2015; Koss et al. 2018). Several dual AGN have been detected locally (Koss et al. 2012; Rubinur et al. 2018; Imanishi et al. 2020), and at higher redshifts (Myers et al. 2008; Hennawi et al. 2010; Silverman et al. 2020; Silva et al. 2021). However, only a few binary AGN have been detected (Kharb et al. 2017).

Galaxy interactions can also lead to triple merger systems, and if the SMBHs of the individual galaxies are accreting, it will form a triple AGN system. Although such systems are rare, a few have been discovered (Koss et al. 2012; Pfeifle et al. 2019). It is important to detect more multiple AGN, in order to understand how AGN activity can affect the merging processes on kpc scales. In this letter, we present the detection of a kpc-scale triple AGN system in a nearby galaxy pair NGC 7733–NGC 7734 (hereafter NGC 7733–34). The instruments, methods and results are described below. The value of Hubble constant (H_0) used in this paper is 67.8 km s^{-1} Mpc^{-1}.

⋆ jyoti [at] iiap.res.in

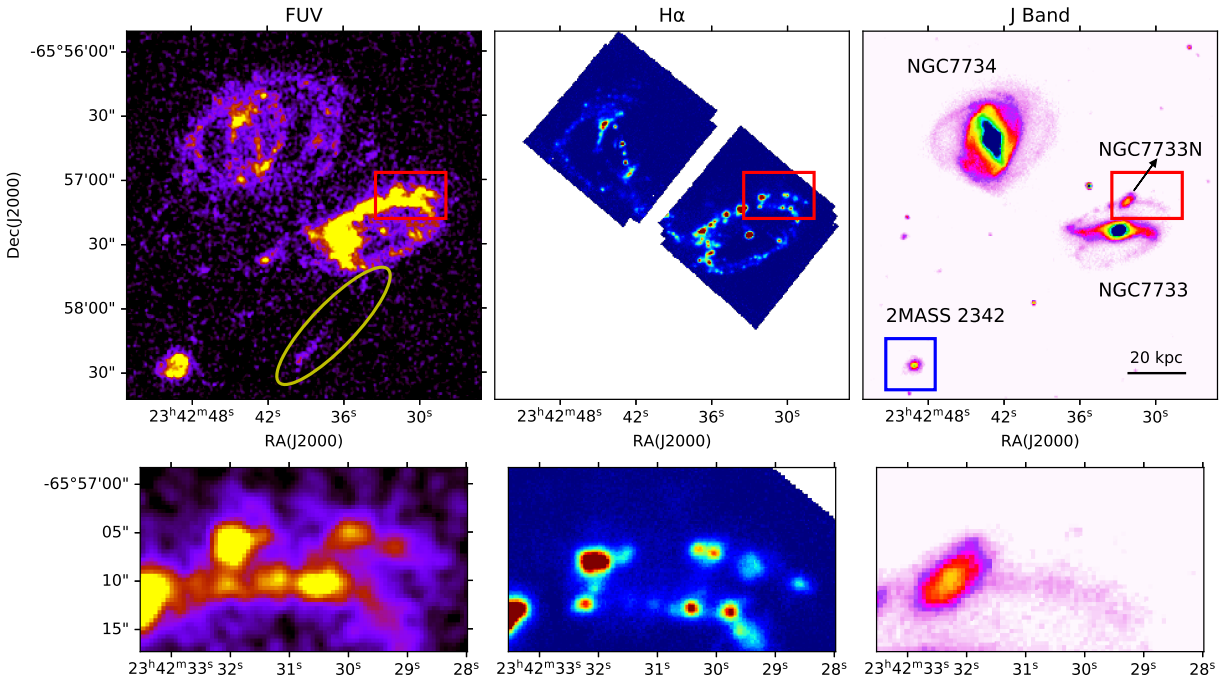

Fig. 1. Upper panel shows the FUV, Hα and J band images of galaxy group NGC 7733–34. Bottom panel shows the zoomed in version of the red rectangles. Blue box represents the possible merging galaxy 2MASS 2342. Yellow ellipse shows the bridge between NGC 7733 and merger candidate 2MASS 2342.

Source	R.A (hh mm ss)	Dec. (dd mm ss)	z
NGC 7733	23:42:32.79	-65:57:27.42	0.03392±0.00003
NGC 7734	23:42:43.20	-65:56:44.19	0.03527±0.00006
NGC 7733N	23:42:32.25	-65:57:09.43	0.03619± 0.00012
2MASS 2342	23:42:49	-65:58:26	

Table 1. Details of the galaxies. Column 2 and 3 are the coordinates of galaxies in J2000.0. Column 4: redshift of NGC 7733 and NGC 7734 taken from Mathewson & Ford (1996) and de Vaucouleurs et al. (1991) respectively.

2. NGC 7733–34 Group

NGC 7733–34 is a group of interacting galaxies at a distance of 154 Mpc (Arp & Madore 1987). NGC7734 is at a distance of 48.3 kpc and has a velocity of 406 km s^{-1} with respect to NGC7733 (de Vaucouleurs et al. 1991). NGC 7733 is a barred spiral that shows knots in the arms and hosts a Seyfert 2 nucleus (Tempel et al. 2016). NGC 7734 is a barred spiral with peculiar arms (de Vaucouleurs et al. 1991; Paturel et al. 1989)). The atomic gas content of the galaxy pair is $\leqslant 4.2 \times 10^9$ M$_\odot$ and the molecular content of NGC 7733 and NGC 7734 is $\leqslant 15.4 \times 10^8$ M$_\odot$ and $\simeq 1.073 \times 10^{10}$ M$_\odot$ respectively (Horellou & Booth 1997). Jahan-Miri & Khosroshahi (2001) identified the star-forming knots and their ages in the individual galaxies and found that NGC 7733 has a much younger stellar population than NGC 7734. The properties of the galaxies are given in Table 1.

3. OBSERVATIONS AND DATA ANALYSIS

3.1. UV DATA

We observed NGC 7733–34 in the far-ultraviolet (FUV) band using the Ultraviolet Imaging Telescope (UVIT) on board ASTROSAT (Kumar et al. 2012). The UVIT has two telescopes that can simultaneously observe in three bands FUV (1300–1800 Å), NUV (2000–3000 Å), and the visible band. Drift correction were done with the visible channel. The UVIT has a spatial resolution of around 1″ and a field of view of 28′. We reduced the UVIT level 1 data downloaded from the Indian Space Science Data Centre (ISSDC) using CCDLAB (Postma & Leahy 2017, 2020).

3.2. Near Infrared DATA

We performed deep Near Infrared (NIR) imaging of the galaxy group NGC 7733–34 with the SIRIUS camera (Nagayama et al. 2003) on the Infrared Survey Facility (IRSF) 1.4 m telescope in Sutherland, South Africa. The SIRIUS camera has three 1024×1024 HgCdTe detectors, which give simultaneous imaging in the J, H, and K bands, with a field of view 7.7′ × 7.7′, and the pixel scale is 0.45″ (Nagayama 2012). The images were taken in automatic dithering mode with ~20″ steps with individual frame exposure times of 30 seconds each, giving a total exposure time of typically ~120 minutes for the combined set of exposures. Data reduction was carried out with a pipeline for the SIRIUS observations, including corrections for non-linearity, dark subtraction, and flat fielding.

3.3. MUSE DATA

We have used Multi Unit Spectroscopic Explorer (MUSE) archival data to study the optical emission lines from NGC 7733–34. MUSE is an integral field spectrograph (IFU) on the Very Large Telescope (VLT) and gives 3D spectroscopic data cubes with very high resolution. We used the data from the wide-field mode, which has a field of view of 1′ × 1′. It has a spatial sampling of 0.2″ × 0.2″ and a spectral resolution of 1750 at 4650Å to 3750 at 9300Å.

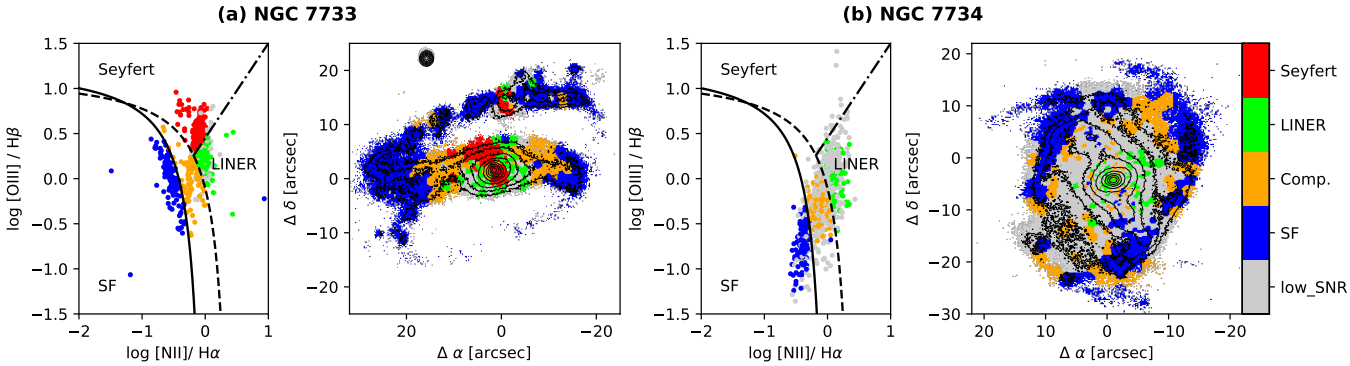

Fig. 2. [N II] BPT Diagrams of NGC 7733 and NGC 7734. $\Delta\alpha$ and $\Delta\delta$ are R.A. and declination with respect to the central position of the source, which is indicated in Table 1. The solid curve in the BPT is taken from Kauffmann et al. (2003), and the region below this line shows the ionization due to star-forming regions. The dashed curve is taken from Kewley et al. (2001), and the region above this line shows the ionization due to AGN. The dashed-dotted line is taken from Schawinski et al. (2007), which divides the LINER and Seyfert AGN. The bins with an amplitude-to-noise (A/N) ratio of less than 4 in any of the lines are shown in gray.

We ran the Galaxy IFU Spectroscopy Tool (GIST[1] version 3.0.3; Bittner et al. 2019) pipeline to analyze the MUSE data. GIST uses a python implemented version of GANDALF (Sarzi et al. 2006; Falcón-Barroso et al. 2006; Bittner et al. 2019) for fitting the gas emission lines and Penalized Pixel-Fitting (pPXF) (Cappellari & Emsellem 2004; Cappellari 2017) method for stellar continuum fitting. GIST gives stellar kinematics and gas emission line properties based on binned data over a given wavelength range and signal-to-noise (S/N). For stellar velocity calculation, the code convolves the linear combination of spectral energy templates with line of sight velocity distribution and fits that with the spectra from each bin.

We have Voronoi binned the data based on Hα (6555–6575 Å) emission. For binning, we used an S/N of 30. We have also corrected the spectra for the Milky Way extinction. We adopted the method used in Comerón et al. (2021) and fitted the continuum using a multiplicative eighth-order Legendre polynomial. We used a minimum S/N of 3 to remove noisy data before binning the data. We have used GIST emission line fluxes for [O III], [N II], Hα and Hβ for further analysis.

Fig. 1 shows the FUV, Hα and NIR J band images of the galaxy group. The FUV and J band images reveal an extended source (2MASS 23424898-6558257 referred to as 2MASS 2342) southeast of the galaxy NGC 7733. The FUV image reveals a bright bridge in the southeastern region connecting NGC 7733 to 2MASS 2342. The extended object in the southeastern region of NGC 7733 could be interacting with NGC 7733 and forms part of the NGC 7733–34 group. The projected spatial separation of 2MASS 2342 from NGC 7733 is ~ 87 kpc assuming that both galaxies are at the same redshift.

4. Nature of the emission from the nuclei in NGC 7733–34

To study the mechanism producing the ionized gas, we derived the BPT plots of the two galaxies (Baldwin et al. 1981). The BPT diagram uses the [O III]λ5007/Hβ and the [N II]λ6563/Hα line ratios to classify the origin of the emission. Fig. 2 (a) and (b) show the BPT plots of NGC 7733 and NGC 7734 respectively. The nuclear emission from NGC 7733 lies in the Seyfert part of the BPT plot, while NGC 7734 shows LINER emission from the central region. The BPT diagram of NGC 7733 also shows the ongoing star formation in the arms and Seyfert-like emission along the minor axis of the bar.

[1] https://abittner.gitlab.io/thegistpipeline/

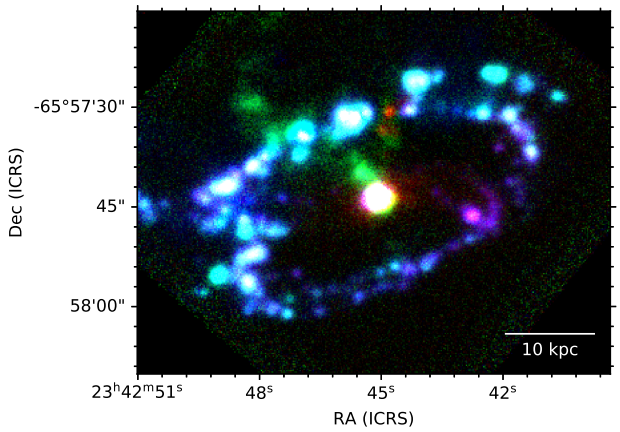

Fig. 3. Color composite Image Of NGC 7733. Blue, green, and red represent the Hα, [O III] and [N II] emissions respectively. The [O III] emission towards the northeastern side shows the ENLR.

Fig. 3 shows the color composite image of Hα (blue), [O III] (green) and [N II] (red) emissions, respectively. The bright Hα emission, in blue along the arms of NGC 7733, confirms the ongoing recent star formation in the arms of the galaxy. The [O III] emission is extended towards the northeast, which confirms that it is due to emission from the extended narrow-line region (ENLR) along the minor axis of the galaxy. The orientation is due to projection effects. The ENLR is associated with photoionized gas around the AGN and can be traced out to ~18 kpc in the northeastern region of NGC 7733. The velocity field and the trailing spirals suggest that the NE side is the near side of the galaxy, so the [O III] emission is extended towards us. The southeastern ENLR is extended away from our line of sight and is not visible due to obscuration by the dust in the galaxy. Ongoing recent star formation activity in NGC 7733 (Jahan-Miri & Khosroshahi 2001) suggests the presence of gas and dust in this galaxy.

5. Is there a third galaxy?

The FUV, J band, and MUSE Hα images show a large bright knot in the northern arm of NGC 7733. This region was identi-

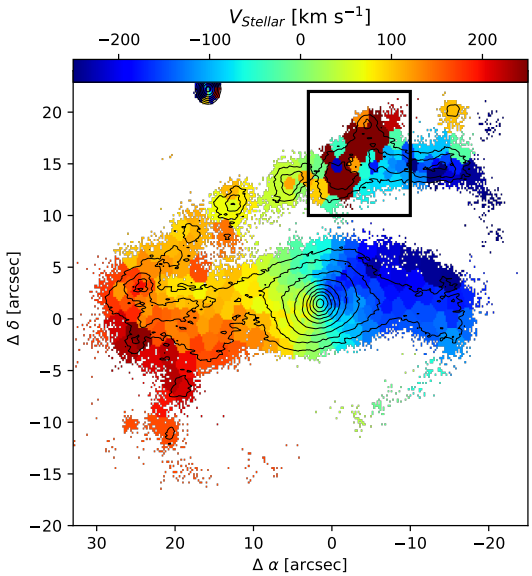

Fig. 4. Stellar velocity map of NGC 7733 obtained from GIST. $\Delta\alpha$ and $\Delta\delta$ are R.A. and Declination with respect to the central position of the source, which is indicated in Table 1. The black rectangle in the northwest shows that the velocity of NGC 7733N is different from galactic rotation.

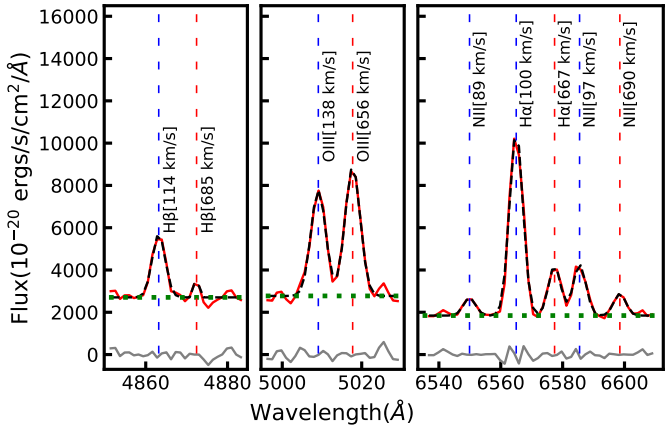

Fig. 5. The blue and red vertical dashed lines correspond to the spectra of NGC 7733 and NGC 7733N, respectively. Observed and fitted spectra are shown in red and black. Continuum is shown by dotted green horizontal lines. The vertical dashed lines show the peaks of emission lines along with their respective velocities.

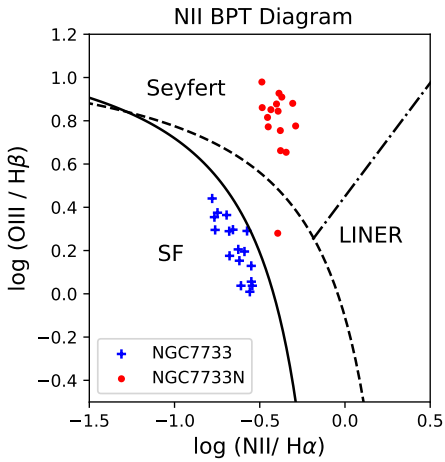

Fig. 6. BPT diagram for NGC 7733 and its companion NGC 7733N. Blue crosses and red dots color represents the emission from NGC 7733 and NGC 7733N respectively.

fied as a star-forming knot in Jahan-Miri & Khosroshahi (2001). The knot appears to be extended in the J band as shown in the red box in Fig. 1. Fig. 4 shows the velocity field of the galaxy NGC 7733. Most of the velocity field shows features typical of a rotating disk, with the Doppler shifted velocities of the approaching (blue) and receding sides (yellow and red). However, the velocity of the knot (shown in the rectangle) is clearly different from the velocity field of the disc.

5.1. Decomposition using GALFIT

We decomposed the NIR images of NGC 7733, and NGC 7734 into bulge, disc, and bar components using GALFIT (Peng et al. 2002) 2-D decomposition code. We modeled both the bulges and the bars using Sersic profiles, and the discs with exponential profiles. A χ^2 minimization technique was used to carry out this fit. We also used the Sersic profile to fit the knot on the northwest arm of NGC 7733 using GALFIT. We found that the effective radius r_e of the Sersic profile in the J band is 3.204″ which corresponds to ~2.4 kpc. Such a large value for the radius of the knot suggests that it is likely to be the bulge of a galaxy, instead of being a star-forming region within NGC 7733.

5.2. Emission line Analysis of the Knot in NGC 7733

The knot shows a different velocity compared to the northern arm of NGC 7733 as indicated by the rectangle in Fig. 4. The MUSE spectra from this region show that there are two sets of emission lines, as shown in Fig. 5. The knot appears to be redshifted by ~650 km s^{-1} with respect to the galaxy. This is a strong indication that the knot is not a part of the galaxy and is instead a separate system that is visually overlapping with the arm of the galaxy. We will use 'NGC 7733N' to refer to the knot in the following text. To check the nature of emission from NGC 7733N, we used the fluxes of Hβ, [O III], Hα and [N II] emission lines for all bins in the rectangle shown in Fig. 4. We divided the spectrum into three wavelength ranges, 4851–4883, 4996–5029, and 6532–6608 Å. We fitted Gaussian profiles to Hβ, [O III], Hα and [N II] lines and a constant continuum as shown in Fig. 5. The emission lines from some of the bins could not be fitted due to poor S/N. The resultant fits confirmed that NGC 7733N has its own set of emission lines. We calculated the mean velocity of Hα in NGC 7733 and NGC 7733N after fitting the emission lines. We found that NGC 7733N is moving with a mean velocity of +655±46 km s^{-1} with respect to NGC 7733 and is at a redshift of 0.03619± 0.00012.

The BPT diagram of two sets of emission lines is shown in Fig. 6. The red markers and blue crosses show the emission from NGC 7733N, and NGC 7733, respectively. The emission from the NGC 7733 component of this region is due to the star formation, which is expected since it originates from the arm. The emission from NGC 7733N lies in the Seyfert region, indicating an AGN in this galaxy.

6. Is this a triple system?

6.1. Tidal features in UV and Hα

Fig. 1 shows an arm-like structure above the main arm in the northern part of NGC 7733 in the UVIT FUV and MUSE Hα images. The arm or tidal tail starts from the western side and merges with the location of NGC 7733N. It is likely to have formed via the tidal interaction between NGC 7733 and NGC 7733N. There are UV and Hα bright knots in the tidal arm, which suggests that there is ongoing massive star formation triggered by the interaction. NGC 7733N then represents the bulge of the merging companion galaxy (Fig. 1), which may have already lost most of its disk mass in the tidal interaction.

6.2. Masses of the central Black holes in NGC 7733, NGC 7733N and NGC 7734

We estimated the K band magnitude and effective radius of the bulges in NGC 7733, NGC 7733N, and NGC 7734 using GALFIT and corrected the magnitude for Galactic extinction using Schlafly & Finkbeiner (2011). We estimated the stellar mass ($M_\star$) of each galaxy using Mass–Luminosity relation (McGaugh & Schombert 2014). Based on the stellar mass ratios, NGC 7733-NGC 7734 is a major while NGC 7733N-NGC 7733 is a minor merging system, respectively. The nuclear black hole masses ($M_\bullet$) were estimated using the following relations; (i) $M_\bullet$–luminosity in the K band (Marconi & Hunt 2003; Kormendy & Ho 2013), (ii) the M–σ relation (Gültekin et al. 2009; McConnell & Ma 2013; Kormendy & Ho 2013) and the (iii) $M_\bullet$–bulge mass relation (Marconi & Hunt 2003; McConnell & Ma 2013; Kormendy & Ho 2013). The SMBH masses for the three AGN and the stellar masses of the galaxies are listed in Table 2. The bulge velocity dispersion of NGC 7733N is not reliable, so we could not calculate the black hole mass in NGC 7733N using the M–σ relation. The nuclear black hole masses of NGC7733 (0.54–4.68 $\times 10^8$ $M_\odot$) and NGC7734 (0.90–3.18 $\times 10^8$ $M_\odot$) have a similar range of values, and their stellar masses are also comparable. NGC 7733N hosts the least massive stellar disk and the least massive nuclear black hole (1.53–5.15 $\times 10^7$ $M_\odot$) in the triple AGN system.

7. Implications for our triple AGN detection

Dual AGN have been detected in many galaxies, but triple AGN are rare. Our study shows that multiple AGN systems can be present in galaxy groups that show ongoing mergers. Since galaxy groups are fairly common (Tempel et al. 2017), they can be good targets for detecting multiple AGN. Another important implication of our study is the enhanced AGN feedback in such systems, which can heat the intra-cluster medium in clusters and enrich the CGM around galaxies (Fabian 2012; Tumlinson et al. 2017). Although multiple AGN feedback is relatively unexplored, it must play an important role in building hot gas reservoirs around galaxies, especially at early epochs when galaxy mergers were more frequent (Lackner et al. 2014; Man et al. 2016; Mundy et al. 2017). Feedback processes such as jets or intense quasar outflows from AGN can affect the evolution of the host galaxy (Salomé et al. 2016; Harrison et al. 2018). Multiple AGN enhance feedback effects may lead to faster SMBH growth (Volonteri et al. 2020). There may be additional star formation if the AGN outflows interact with each other. Triple AGN systems such as the one we have detected in NGC 7733–34 are thus ideal laboratories to study the growth of hot gas, AGN feedback, and SMBH growth in mergers and should be relatively common in gas-rich galaxy groups.

8. Conclusions

1. We find that the paired galaxies NGC 7733 and NGC 7734 host Liner and Seyfert type nuclei, respectively.
2. We also detected an ENLR from the AGN in NGC 7733 towards the northeastern region.
3. The multiwavelength data shows a tidal arm above the northern arm of NGC 7733, and the tidal arm connects with the location of a third galaxy which we call NGC 7733N.
4. We have confirmed the existence of the third galaxy NGC 7733N in the NGC 7733–34 group. It appears to overlap with the northern arm of NGC 7733. The emission line analysis of NGC 7733N shows that it hosts a Seyfert nucleus.
5. The UV and NIR images show a fourth galaxy (2MASS 2342) lying southeast of the galaxy pair, which could be part of the merging system. We see a potential bridge between NGC 7733 and 2MASS 2342 in the UV map. This bridge is composed of hot gas that has been pulled out during the interaction phase. However, redshift estimation is necessary to confirm this.

Triple-AGN are rare, however, detailed studies could enhance their observed frequency in groups, and especially at high redshift. Although this study focuses only on one system, the results suggest that small merging groups are ideal laboratories to study multiple AGN systems.

Acknowledgements. We thank the anonymous referee for the thoughtful review, which improved the impact and clarity of this work. This publication uses the data from the UVIT, which is part of the AstroSat mission of the Indian Space Research Organisation (ISRO), archived at the Indian Space Science Data Centre (ISSDC). This research has also used NIR data from IRSF at the South African Astronomical Observatory (SAAO). Part of the results are based on observations collected at the European Southern Observatory under ESO programme 0103.A-0637, run B. This research has made use of the NASA/IPAC Extragalactic Database (NED) which is operated by the Jet Propulsion Laboratory, California Institute of Technology, under contract with the National Aeronautics and Space Administration. M.D. acknowledges the support of Science and Engineering Research Board (SERB) MATRICS grant MTR/2020/000266 for this research.

References

Arnold, T. J., Martini, P., Mulchaey, J. S., Berti, A., & Jeltema, T. E. 2009, ApJ, 707, 1691
Arp, H. C. & Madore, B. 1987, A catalogue of southern peculiar galaxies and associations
Baldwin, J. A., Phillips, M. M., & Terlevich, R. 1981, PASP, 93, 5
Bittner, A., Falcón-Barroso, J., Nedelchev, B., et al. 2019, A&A, 628, A117
Cappellari, M. 2017, MNRAS, 466, 798
Cappellari, M. & Emsellem, E. 2004, PASP, 116, 138
Combes, F. 2001, in Advanced Lectures on the Starburst-AGN, ed. I. Aretxaga, D. Kunth, & R. Mújica, 223
Comerón, S., Knapen, J. H., Ramos Almeida, C., & Watkins, A. E. 2021, A&A, 645, A130
de Vaucouleurs, G., de Vaucouleurs, A., Corwin, Herold G., J., et al. 1991, Third Reference Catalogue of Bright Galaxies
Di Matteo, T., Springel, V., & Hernquist, L. 2005, Nature, 433, 604
Duc, P.-A. & Renaud, F. 2013, Tides in Colliding Galaxies, ed. J. Souchay, S. Mathis, & T. Tokieda, Vol. 861, 327
Eastman, J., Martini, P., Sivakoff, G., et al. 2007, ApJ, 664, L9
Fabian, A. C. 2012, ARA&A, 50, 455
Falcón-Barroso, J., Bacon, R., Bureau, M., et al. 2006, MNRAS, 369, 529
Georgakakis, A., Gerke, B. F., Nandra, K., et al. 2008, MNRAS, 391, 183
Gültekin, K., Richstone, D. O., Gebhardt, K., et al. 2009, ApJ, 698, 198
Harrison, C. M., Costa, T., Tadhunter, C. N., et al. 2018, Nature Astronomy, 2, 198
Hennawi, J. F., Myers, A. D., Shen, Y., et al. 2010, ApJ, 719, 1672

Galaxy	M_K (mag)	Re (arcsec)	$\log(M_\star)$	Black Hole Mass (10^8 $M_\odot$)							
				$M_\bullet$–L_K		$M_\bullet$–σ			$M_\bullet$-M_{bulge}		
				MH2003	KH2013	Gu2009	MM2013	KH2013	MH2003	MM2013	KH2013
NGC 7733	-24.09	1.73	11.39	$1.83^{+0.62}_{-0.43}$	$4.68^{+1.14}_{-1.03}$	$0.54^{+0.05}_{-0.05}$	$0.64^{+0.03}_{-0.03}$	$1.24^{+0.06}_{-0.07}$	$1.31^{+0.89}_{-0.31}$	$1.86^{+0.73}_{-0.56}$	$3.04^{+0.91}_{-0.73}$
NGC 7734	-23.74	1.58	11.81	$1.28^{+0.36}_{-0.26}$	$3.18^{+0.90}_{-0.77}$	$1.13^{+0.20}_{-0.18}$	$1.70^{+0.18}_{-0.17}$	$2.63^{+0.28}_{-0.26}$	$0.90^{+0.60}_{-0.21}$	$1.25^{+0.57}_{-0.41}$	$1.98^{+0.67}_{-0.52}$
NGC 7733N	-22.11	3.1	9.96	$0.23^{+0.01}_{-0.01}$	$0.51^{+0.24}_{-0.17}$				$0.15^{+0.10}_{-0.04}$	$0.19^{+0.14}_{-0.09}$	$0.26^{+0.14}_{-0.09}$

Table 2. Properties of Galactic Bulges and central black holes. Column 2: K band Absolute magnitude of bulges. Column 3: Effective radius of bulges. Column 4: Stellar mass estimated in K band using $M/L = 0.6$ (McGaugh & Schombert 2014). Column 5 and 6: Mass of central black holes using $M_\bullet$ and K band luminosity. Column 7, 8 and 9: Mass of central black holes using $M_\bullet$–σ relation. Column 10, 11 and 12: Mass of central black holes using $M_\bullet$– Mass of bulge relation. MH2003: Marconi & Hunt (2003), KH2013: Kormendy & Ho (2013), Gu2009: Gültekin et al. (2009), MM2013: McConnell & Ma (2013).

Hopkins, P. F. & Quataert, E. 2011, MNRAS, 415, 1027
Horellou, C. & Booth, R. 1997, A&AS, 126, 3
Imanishi, M., Kawamuro, T., Kikuta, S., Nakano, S., & Saito, Y. 2020, ApJ, 891, 140
Jahan-Miri, M. & Khosroshahi, H. G. 2001, AJ, 122, 792
Kauffmann, G., Heckman, T. M., Tremonti, C., et al. 2003, MNRAS, 346, 1055
Kenney, J. D. P., van Gorkom, J. H., & Vollmer, B. 2004, AJ, 127, 3361
Kewley, L. J., Dopita, M. A., Sutherland, R. S., Heisler, C. A., & Trevena, J. 2001, ApJ, 556, 121
Kharb, P., Lal, D. V., & Merritt, D. 2017, Nature Astronomy, 1, 727
Kocevski, D. D., Brightman, M., Koekemoer, A. M., & Nandra, K. 2015, Are Compton-Thick AGN the Missing Link Between Mergers and Black Hole Growth?, HST Proposal
Kormendy, J. & Ho, L. C. 2013, ARA&A, 51, 511
Koss, M., Mushotzky, R., Treister, E., et al. 2012, ApJ, 746, L22
Koss, M. J., Blecha, L., Bernhard, P., et al. 2018, Nature, 563, 214
Kumar, A., Ghosh, S. K., Hutchings, J., et al. 2012, in Society of Photo-Optical Instrumentation Engineers (SPIE) Conference Series, Vol. 8443, Space Telescopes and Instrumentation 2012: Ultraviolet to Gamma Ray, ed. T. Takahashi, S. S. Murray, & J.-W. A. den Herder, 84431N
Lackner, C. N., Silverman, J. D., Salvato, M., et al. 2014, AJ, 148, 137
Man, A. W. S., Zirm, A. W., & Toft, S. 2016, ApJ, 830, 89
Marconi, A. & Hunt, L. K. 2003, ApJ, 589, L21
Martini, P., Sivakoff, G. R., & Mulchaey, J. S. 2009, ApJ, 701, 66
Mathewson, D. S. & Ford, V. L. 1996, ApJS, 107, 97
McConnell, N. J. & Ma, C.-P. 2013, ApJ, 764, 184
McGaugh, S. S. & Schombert, J. M. 2014, AJ, 148, 77
McGee, S. L., Balogh, M. L., Bower, R. G., Font, A. S., & McCarthy, I. G. 2009, MNRAS, 400, 937
Mundy, C. J., Conselice, C. J., Duncan, K. J., et al. 2017, MNRAS, 470, 3507
Myers, A. D., Richards, G. T., Brunner, R. J., et al. 2008, ApJ, 678, 635
Nagayama, T. 2012, African Skies, 16, 98
Nagayama, T., Nagashima, C., Nakajima, Y., et al. 2003, in Society of Photo-Optical Instrumentation Engineers (SPIE) Conference Series, Vol. 4841, Instrument Design and Performance for Optical/Infrared Ground-based Telescopes, ed. M. Iye & A. F. M. Moorwood, 459–464
Paturel, G., Fouque, P., Bottinelli, L., & Gouguenheim, L. 1989, A&AS, 80, 299
Peng, C. Y., Ho, L. C., Impey, C. D., & Rix, H.-W. 2002, AJ, 124, 266
Pfeifle, R. W., Satyapal, S., Manzano-King, C., et al. 2019, ApJ, 883, 167
Postma, J. E. & Leahy, D. 2017, PASP, 129, 115002
Postma, J. E. & Leahy, D. 2020, PASP, 132, 054503
Rubinur, K., Das, M., & Kharb, P. 2018, Journal of Astrophysics and Astronomy, 39, 8
Rubinur, K., Das, M., & Kharb, P. 2019, MNRAS, 484, 4933
Salomé, Q., Salomé, P., Combes, F., & Hamer, S. 2016, A&A, 595, A65
Sarzi, M., Falcón-Barroso, J., Davies, R. L., et al. 2006, MNRAS, 366, 1151
Satyapal, S., Ellison, S. L., McAlpine, W., et al. 2014, MNRAS, 441, 1297
Schawinski, K., Thomas, D., Sarzi, M., et al. 2007, MNRAS, 382, 1415
Schlafly, E. F. & Finkbeiner, D. P. 2011, ApJ, 737, 103
Silva, A., Marchesini, D., Silverman, J. D., et al. 2021, ApJ, 909, 124
Silverman, J. D., Tang, S., Lee, K.-G., et al. 2020, ApJ, 899, 154
Springel, V., Di Matteo, T., & Hernquist, L. 2005, ApJ, 620, L79
Tempel, E., Kipper, R., Tamm, A., et al. 2016, A&A, 588, A14
Tempel, E., Tuvikene, T., Kipper, R., & Libeskind, N. I. 2017, A&A, 602, A100
Tumlinson, J., Peeples, M. S., & Werk, J. K. 2017, ARA&A, 55, 389
Tzanavaris, P., Gallagher, S. C., Hornschemeier, A. E., et al. 2014, ApJS, 212, 9
Volonteri, M., Pfister, H., Beckmann, R. S., et al. 2020, MNRAS, 498, 2219
von der Linden, A., Wild, V., Kauffmann, G., White, S. D. M., & Weinmann, S. 2010, MNRAS, 404, 1231
Yadav, J., Das, M., Patra, N. N., et al. 2021, ApJ, 914, 54